4-ISOQUINOLINEBORONIC ACID: THEORETICAL AND EXPERIMENTAL STUDIES USING FT-IR, UV-VISIBLE, FLUORESCENCE SPECTRA WITH THE HELP OF DFT METHOD

[1]Katta Eswar Srikanth, [2]A.Veeraiah

[1]Molecular spectroscopy laboratory, Department of Physics, D.N.R.College(A), Bhimavaram, A.P., India-534 202.

Abstract: In this investigation the FT-IR spectrum was recorded in the region 400-4000 cm^{-1}. Potential energy surface (PES) scan analysis was carried out to the titled compound in order to know the stable conformer with the help of potential energy profile. The stable conformer of the titled was optimized at B3LYP functional with 6-311++G** basis set. There after we calculated the theoretical frequencies, IR intensities, and bonding parameters of the examined compound by using DFT/6-311++G** basis set. In Gaussian output file there was no imaginary frequencies i.e. negative frequencies, so we concluded that the titled compound was optimized very well. For this structure we calculated the bond lengths, angles and dihedral angles theoretically and compared with the experimentally available data of similar type structure. In order to know the Hydrogen bonding interactions, π-π interactions and charge transfer within the molecule NBO investigation was performed to the titled compound. NLO and frontier molecular orbital analysis was also carried out using 6-311++G** basis set. TD-DFT calculations were carried out to support the experimental results of the titled compound. Molecular electrostatic potential maps (MEP), thermodynamic properties, Mulliken atomic charge population analysis was also carried to the titled compound.

IndexTerms **- 4-Isoquinolineboronic acid (4IQBA), FT-IR, UV-Vis spectra, fluorescence spectra.**

I. INTRODUCTION

Isoquinoline belongs to heterocyclic aromatic compound and have many applications in synthetic organic chemistry. It is the structural isomer of quinolone. Its structure is made up of benzene ring fused with pyridine ring and hence these are also known as benzopyridines. Isoquinoline obtains from natural products like amino acid tyrosine which is also an aromatic compound [1-6]. Isoquinoline derivatives shows activity and these are used as treatment for anti-malarial [7], anti-hypertensive [8], antifungal [9], anti-microbial [10], anti-tumor [11], anti-diabetic, anti-oxidant and anti-hypertensive [12]. In addition to that isoquinoline derivatives also used as building blocks in medicinal industry and pharmaceuticals [13-15]. Isoquinolines are present in different proportions in prickly poopy, bloodroot and celandine poppy [16-17]. The most important properties of Amino-quinolone derivatives are used as prevention of human immuno deficiency virus (HIV) [18] and also used for the treatment of erythrocytic plasmodial infections [19] 4-amino-7-chloroquinoline shows good antimalarial activity [20]. Two of the Isoquinoline derivatives namely 5-substituted isoquinoline-1-ones and 3,4-dihydro-5-[4-(1-piperidinyl)-butoxy]-1(2H)-isoquinolinone (DPQ) are effective preventer of poly(ADP-ribose) polymerase (PARP—which is an enzyme that plays a crucial role in polymerizing ADP-ribose in DNA backbone synthesis) [21-22]. To our knowledge vibrational analysis and theoretical quantum chemical calculations of 4-Isoquinolineboronic acid have not been reported. In this paper we reported the vibrational spectra, electronic absorption spectra, fluorescence spectra, NBO analysis, NLO analysis, frontier molecular orbitals and corresponding HOMO-LUMO gap, chemical reactive descriptors, Mulliken atomic charge population analysis and thermodynamic properties for the first time.

II. Experimental details:

4-Isoquinolineboronic acid specimen in the solid state was procured from Sigma-Aldrich Chemical Company with a stated purity of 97% and it was used for spectral measurements without further purification.

2.1 FT-IR Spectrum:

Fourier transform Infrared spectrum of the compound is recorded at 299.15^0 K temperature in the region 4000-400 cm^{-1} using Nicolet 6700 FT-IR spectrometer assembled with a Thermo Nicolet Continuous IR microscope or high performance single bound diamond attenuated total reflectance (ATR) accessory and by a Reni Shaw in via., Raman microscope with UV or visible laser excitation at a resolution of 4 cm^{-1}.

2.2 UV-Vis and Fluorescence spectrum:

Electronic spectrum of the examined compound was measured in the range of 300-1100 nm utilizing a Perkin Elmer Lambda 35 UV-Vis spectrometer. Experimental data was recorded after 1 cycle, with an interval of 1 nm, slit width of 2 nm and scan speed of 240 $nm\text{-}min^{-1}$ with the spectral resolution of 0.05-4.0 nm. Fluorescence and UV-Vis spectrum were recorded using methanol as solvent. The slit width was set to 15 nm for the excitation monochromator and to 10 nm for the emission monochromator.

III. Computational Details:

The potential energy surface (PES) scan of the investigated compound has been predicted as function of dihedral angle by employing B3LYP/6−311++G** method to find out the stable conformers. The obtained stable conformer have been optimized and vibrational frequencies of (4IQBA) was calculated using Becke-3-Lee Yang Parr (B3LYP) at DFT/B3LYP/6-311++G** standard basis set by using Gaussian 09W program package [23]. The Cartesian presentation of the computed force constants has been calculated at the most optimized geometry in the ground state. The multiple scaling of the force constants of the titled

compound were performed by the quantum chemical method with selective scaling in the local symmetry coordinates representations [24], utilizing transferable scale factors available in the literature [25]. The transformation of force field from Cartesian to symmetry coordinate, the scaling, the subsequent normal coordinate analysis, calculations of PED and IR intensities were calculated on a Personal Computer with the version V7.0-G77 of the MOLVIB program written by Sundius [26, 27]. In order to attain a close coincidence between observed and calculated frequencies, the least square fit refinement algorithm was used. Thereafter, the reactive site of the molecule was examined with the help of the molecular electrostatic potential (MESP) Map. In order to show the non-linear optical (NLO) activity of the molecule, the linear polarizability, dipole moment and first order hyper polarizability are obtained by molecular polarizabilities by using GAUSSIAN09W with the same level of theory. Also, the frontier molecular orbital (FMO) calculations also carried out because of their interrelation with the non-linear optical activity of the investigated molecule.

IV. Results and Discussion

4.1 PES Scan:

The potential energy surface (PES) scan with the DFT/B3LYP/6-311++G** level of theoretical calculations were carried out to the investigated molecule which was represented in Fig. 1. The dihedral angle C8–C7–B11–O12 for 4IQBA was also the suitable coordinate for conformational flexibility within the molecule. Throughout the calculations all the geometrical parameters like dihedral angles were simultaneously relaxed during the calculations while the C1–O11–C12–C13 dihedral angle was differed in steps of 10º, 20º, 30º, ..., 200º. At the 10^0 rotation, minimum energy curve has been achieved for C8–C7–B11–O12. The energy barrier of this rotation at 10º angle is Hartrees.

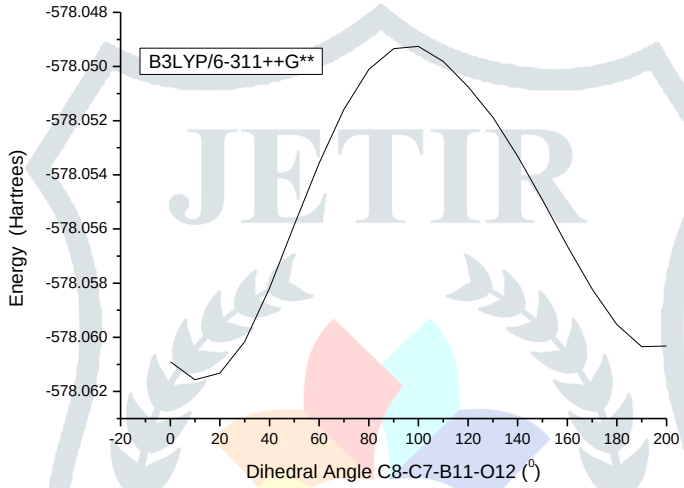

Fig.1: Potential energy surface scan for dihedral angle C8-C7-B11-O12 of 4-Isoquinolineboronic acid

4.2 Optimized structural parameters:

The optimized molecular structure of the titled compound 4-Isoquinolineboronic acid (4IQBA) belongs to C_1 point group symmetry and it was shown in Fig.2. The optimized structural comparative parameters such as bond lengths and bond angles calculated at B3LYP/6-311++G** method of the titled compound are presented in Table 1. From the table, theoretical results shows that the Isoquinoline ring in 4IQBA is little distorted this is due to the electronic effect of the substituent groups. To the best of our knowledge, exact experimental data on the geometrical parameters of title compound are not available in the literature. So, for comparative purpose we use the crystal structure of closely related molecules [28-29]. From the table, we observed that there is a difference between theoretical and experimental data because crystalline state involved in hydrogen bonding but theoretical values obtained from gas phase medium. Thereafter, it was noticed that the maximum deviation between the theoretical and XRD data was 0.214 Å for O12-H20, 0.213 Å for O13-H21 and 0.004 to 0.15Å for other bond lengths. In the case of bond angles the deviation varies between 0° to 5°. The maximum deviation between theoretical and experimental bond angle O12-B11-O13 was 5° and there is a good coincidence between the experimental and theoretical bond angles for N9-C10-C5, C10-C5-C6, C1-C2-H15, C4-C3-H16 and C7-C8-H18. The order of theoretical bond angles were O13-B11-O12>B11-C7-C6≈C7-B11-O13≈N9-C8-H18≈B11-O12-H20>C6-C7-C8. In spite of theoretical results are not accurately equal to the XRD values for this compound, they are probably accepted that bond lengths and bond angles depend on the method of theory and the basis set used in the calculations, and they can be used as support to calculate the molecular properties for the investigated molecules.

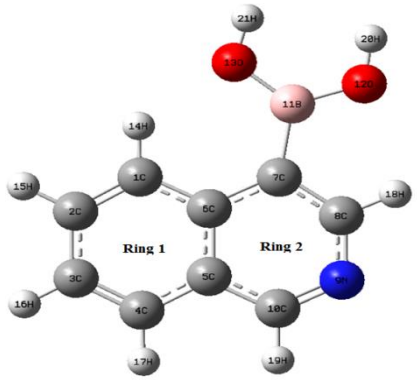

Fig.2: Optimized Molecular structure of 4-IQBA along with numbering of atom.

Table 1: Optimized geometrical parameters of 4IQBA obtained by B3LYP/6-311++G** density functional calculations

	Value(Å)			Value(°)	
Bond length	6-311++G**	Exp*	Bond Angle	6-311++G**	Exp*
C1-C2	1.378	1.37[a]	C1-C2-C3	122	123[a]
C2-C3	1.415	1.39[a]	C2-C3-C4	120	121[a]
C3-C4	1.374	1.37[a]	C3-C4-C5	120	119[a]
C4-C5	1.418	1.40[a]	C4-C5-C6	121	122[a]
C5-C6	1.431	1.41[a]	C6-C1-C2	120	118[a]
C6-C1	1.423	1.44[a]	C6-C7-C8	117	120[a]
C6-C7	1.438	1.40[a]	C7-C8-N9	126	123[a]
C7-C8	1.389	1.35[a]	N9-C10-C5	124	124[a]
C10-C5	1.419	1.42[a]	C10-C5-C6	118	118[a]
C8-N9	1.359	1.37[a]	B11-C7-C8	117	120[b]
C10-N9	1.316	1.31[a]	B11-C7-C6	126	122[b]
C7-B11	1.569	1.56[b]	C7-B11-O12	117	118[b]
B11-O12	1.374	1.37[b]	C7-B11-O13	121	125[b]
B11-O13	1.375	1.36[b]	O13-B11-O12	122	117[b]
O12-H20	0.963	0.75[b]	C6-C1-H14	119	--
O13-H21	0.964	0.75[b]	C2-C1-H14	120	--
C1-H14	1.081	0.93[a]	C1-C2-H15	119	119[a]
C2-H15	1.086	0.93[a]	C3-C2-H15	119	--
C3-H16	1.085	0.93[a]	C2-C3-H16	119	--
C4-H17	1.087	0.93[a]	C4-C3-H16	120	120[a]
C8-H18	1.086	0.93[a]	C3-C4-H17	121	120[a]
C10-H19	1.091	0.93[a]	C5-C4-H17	119	119[a]
			N9-C8-H18	115	119[a]
			C7-C8-H18	119	119[a]
			C5-C10-H19	118	--
			N9-C10-H19	117	119[a]
			B11-O12-H20	115	111[b]
			B11-O13-H21	114	111[b]

[a] see reference [28]
[b] see reference [29]

4.3 Vibrational frequency analysis:

The titled molecule was a non-planar and having 21 atoms therefore it shows 3N-6 (N = no of atoms present in the molecule) i.e. 57 potentially active fundamental modes of vibrations under C_1 point group symmetry. It can be represented as follows

$$\Gamma 3N-6 = 39A' (in-plane) + 18A'' (out-of-plane)$$

Normal coordinate analysis (NCA) gives the detailed information about the vibrational assignments of the compound under investigation. The particular assignment to the each and every individual frequency is assigned by potential energy distribution (PED) analysis. So we defined a full set of internal coordinates which is shown in supplementary material 1. In order to obtain the normal modes in a coordinate system, the internal coordinates can be reduced in to local symmetry coordinated from the recommendations of Fogarasi and Pulay [30-31] which are presented in Table 2. PED method also shows that the mixing of other modes contribution to normal mode of vibration. Most probably the maximum contribution is agreed to be the most suitable mode. The complete analysis of fundamental modes of vibration with FT-IR experimental frequencies, scaled vibrational frequencies, IR intensities and PED of 4IQBA using B3LYP method with 6-311++G** basis set are shown in Table 3. All the vibrations are active in IR. The experimental FT-IR spectrum with corresponding theoretically simulated FT-IR spectrum for 4IQBA are shown in Figs.3.

Table 2: Definition of local-symmetry coordinates and the values of corresponding scale factors used to correct the B3LYP/6-311++G** (refined) force field of 4IQBA

No.(i)	Symbol [a]	Definition[b]	Scale factors
Stretching			
1 to 6	ν(C-H)	R1, R2, R3, R4, R5,R6	0.953
7-15	ν(C-C)ar	R7, R8, R9, R10, R11, R12, R13,R14,R15	0.999
16-17	ν(C-N)ring2	R16,R17	0.999
18	ν(C-B)sub	R18	0.999
19	ν(B-O)ss	(R19+R20)/√2	0.978
20	ν(B-O)ass	(R19-R20)/√2	0.978
21-22	ν(O-H)sub	R21,R22	0.851
In-Plane bending			

23-28	β_{C-H}	(γ23- γ24)/√2, (γ25-γ26)/√2, (γ27-γ28)/√2, (γ 29-γ30)/√2, (γ 31-γ32)/√2, (γ 33-γ34)/√2	1.015
29-30	βRtri	(γ 35-γ 36+ γ37-γ 38+ γ39-γ40)/√6, (γ 41-γ 42+ γ43-γ 44+ γ45-γ46)/√6	0.982
31-32	βRasy	(2γ 35-γ 36- γ37+2γ38- γ39-γ40)/√12, (2γ 41-γ 42- γ43+2γ44- γ45-γ46)/√12	0.982
33-34	βRsym	(γ 36- γ37+ γ39-γ40)/2, (γ 42- γ43+ γ45-γ46)/2	0.982
35	βBC	(γ 47-γ48)/√2	0.995
36	βCBO	(γ 49-γ50)/√2	0.936
37-38	βBOH	γ 51, γ52	0.994
39	βBO_2	(2γ55-γ54- γ53)/√6	0.936
Out of plane bending			
40-45	ωC-H	ρ56, ρ57, ρ58, ρ59, ρ 60, ρ61	0.977
46	ωC-B	ρ62	0.983
47	ωO-C	ρ63	0.983
Torsions			
48	τOBCC	(τ 64- τ 65)/2	1.042
49	τR1tri	(τ 66-τ67+τ68-τ69+τ70-τ71)/√6	0.931
50	τR2tri	(τ 72-τ73+τ74-τ75+τ76-τ77)/√6	0.999
51	τR1asy	(τ 66-τ68+τ69-τ71)/2	0.931
52	τR2asy	(τ 72-τ74+τ75-τ77)/2	0.999
53	τR1sym	(-τ66-2τ67-τ68+τ69+2τ70-τ71)√12	0.931
54	τR2sym	(-τ72-2τ73-τ74+τ75+2τ76-τ77)√12	0.999
55	τOBOH	(τ78-τ79)/2	1.042
56	τCBOH	(τ80-τ81)/2	1.042
57	Butter	(τ82-τ83)/2	0.936

Where a=cos144^0, b=cos72^0.

Abbreviations: ν, stretching; β, in plane bending; ω, out of plane bending; τ, torsion, ss, symmetrical stretching, ass, asymmetrical stretching, tri, trigonal deformation, sym, symmetrical deformation, asy, asymmetric deformation, butter, butterfly, ar, aromatic, sub, substitution.

[a] These symbols are used for description of the normal modes by PED in Table 3.

[b] The internal coordinates used here are defined in table given in supplementary material 1

Supplementary material 1: Definition of internal coordinates of 4-Isoquinolineboronic acid

No.(i)	Symbol	Type	Definition [a]
Stretching			
1-6	R_i	CH(Ring)	C1-H14,C2-H15,C3-H16,C4-H17,C10-H19,C8-H18
7-12	R_i	CC(ring1)	C1-C2,C2-C3,C3-C4,C4-C5,C5-C6,C6-C1
13-15	R_i	CC(ring2)	C6-C7,C7-C8,C10-C5
16-17	R_i	CN(Ring2)	C8-N9,C10-N9
18	R_i	CBsub	C7-B11
19-20	R_i	BOsub	B11-O12,B11-O13
21-22	Ri	OHsub	O13-H21,O12-H20
In-Plane bending			
23-34	γi	CCH(Ring1)	C6-C1-H14,C2-C1-H14,C1-C2-H15,C3-C2-H15,C2-C3-H16,C4-C3-H16,C3-C4-H17,C5-C4-H17,C5-C10-H19,N9-C10-H19,N9-C8-H18,C7-C8-H18
35-40	γi	Ring1	C1-C2-C3,C2-C3-C4,C3-C4-C5,C4-C5-C6,C5-C6-C7,C6-C1-C2
41-46	γi	Ring2	C6-C7-C8,C7-C8-N9,N9-C10-C5,C10-C5-C6,C5-C6-C7,C6-C7-C8
47-48	γi	BCsub	B11-C7-C8,B11-C7-C6
49-50	γi	CBOsub	C7-B11-O12,C7-B11-O13
51-52	γi	BOHsub	B11-O13-H21,B11-O12-H20
53-54	γi	CBO(sub)	C7-B11-O13,C7-B11-O12
55	γi	OBO	O13-B11-O12
Out-of-plane bending			
56-61	ρi	CH	H14-C1-C2-C6,H15-C2-C1-C3,H16-C3-C2-C4,H17-C4-C3-C5,H19-C10-C5-N9,H18-C8-C7-N9
62	ρi	CB	B11-C7-C6-C8
63		OC	C7-B11-O12-O13
Torsion			
64-65	τi	OBCC	O12-B11-C7-C8, O12-B11-C7-C6.
66-71	τi	RING 1	C1-C2-C3-C4, C2-C3-C4-C5, C3-C4-C5-C6, C4-C5-C6-C1, C5-C6-C1-C2, C6-C1-C2-C3
72-77	τi	RING2	C6-C7-C8-N9,C7-C8-N9-C10,C8-N9-C10-C5,N9-C10-C5-C6,C10-C5-C6-C7,C5-C6-C7-C8
78-79	τi	OBOH	O13-B11-O12-H20, O12-B11-O13-H21

80-81		CBOH	C7-B11-O12-H20, C7-B11-O13-H21
82-83	τi	Butterfly	C4-C5-C6-C7,C10-C5-C6-C1

[a] For numbering of atom refer Fig.2

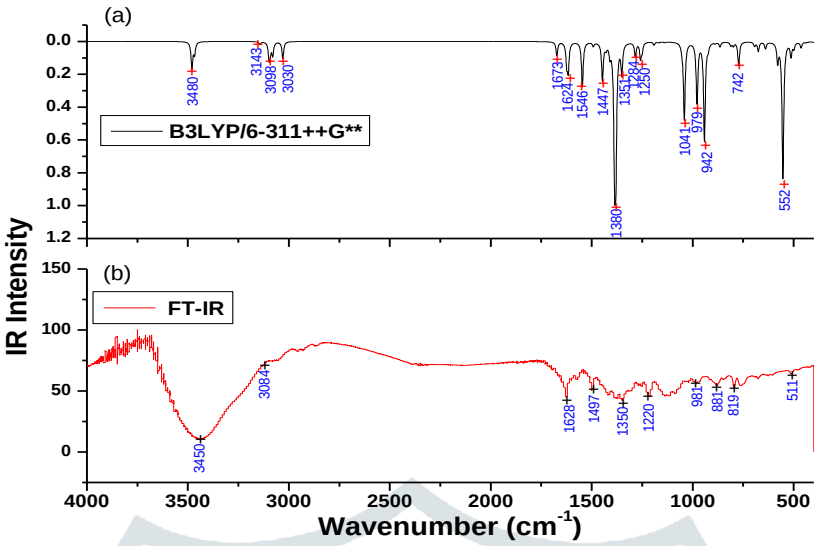

Fig.3: (a) Simulated, (b) Experimental FT-IR spectrum of 4-IQBA

4.3.1 C-H vibrations:

Generally, aromatic compounds shows multiple weak bands in the region 3100-3000 cm^{-1} due to aromatic C-H stretching vibrations [32-34]. In this paper, The weak absorption bands observed at 3178cm^{-1}, 3090cm^{-1}, 3084cm^{-1}, 3070cm^{-1}, 3056cm^{-1} in FT-IR spectrum was assigned to C-H stretching modes of vibrations. Thereafter, the C-H in plane bending vibrations lies in the region 1290-900 cm^{-1} for the benzene and allied molecules [35-36]. Generally these bands are weak to moderate intensity. In this compound the weak band at 1284, medium strong band at 1252, weak band at 1190, 1169, 1140 and 1083 cm^{-1} assigned for the C-H in plane bending vibrations with corresponding theoretical values at 1282, 1249, 1191, 1167, 1138 and 1052cm^{-1} obtained from DFT/B3LYP/6-311++G** method of theory. Very good coincidences between theoretical and observed values were achieved.

The C-H out of plane bending vibrations depends upon the nature of the neighboring hydrogen atoms and not much influenced by the substituent present in the molecule. These vibrations are strongly coupled with neighboring atoms [37]. The C-H out of plane bending vibrations observed in the region 1000- 600 cm^{-1} for small poly aromatic hydrocarbons [38-39]. Now coming to the present compound, the weak bands observed at 1007, 995, 981, medium strong band at 914, weak band at 880 and very weak band at 780 in FT-IR spectrum was assigned to C-H out of plane bending vibrations. So from the above discussion we concluded that all the vibrations lie within the characteristic region.

4.3.2 Ring vibrations:

Most probably, the C-C stretching vibrations occurred in the characteristic region of 1625-1200 cm^{-1}. In the present study, the bands observed at 1675(vw), 1545(w), 1497(ms), 1459(w), 1420(ms), 1402 (w) in FT-IR spectrum was assigned to C=C stretching frequency for the titled compound which are non-degenarate and those weak bands observed at 1352, 1266 in FT-IR spectrum was assigned to C-C stretching frequency which are degenerate modes of vibrations. Similarly, the peaks observed at 856(ms), 819(w), 511(w) in FT-IR spectrum was assigned to C-C-C in-plane bending vibrations for pyridine derivative present in the Isoquinoline and the medium strong peak observed at 646 was assigned to C-C-C out of plane bending vibrations for pyridine derivative. Thereafter, the bands observed at 685(w), 573 (vw) 557(w) in FT-IR spectrum was assigned to in-plane bending vibration of benzene derivative of isoquinoline and the bands at 795(w), 492 (vw) and 492(vw) in FT-IR spectrum was assigned to C-C-C out of plane bending vibrations.

4.3.3 C-N vibrations:

The assignment of C-N stretching frequency was very difficult task due to mixing of other modes in the region 1600-1400 cm^{-1}. So by using normal coordinate analysis and potential energy distribution analysis we can assign the theoretical C-N stretching frequency at 1626cm^{-1} and 1616 which are supported by the medium strong band at 1628 and weak band at 1608 in FT-IR spectrum.

4.3.4 B-O vibrations:

Generally, the B-O asymmetric stretching vibration was observed in the region 1390-1330 cm^{-1} for phenylboronic acid [40-42]. In the target molecule theoretical B-O asymmetric stretching vibration was scaled at 1386 which was confirmed by the medium strong bond at 1380 in FT-IR spectrum. The B-O symmetric stretching vibrations lies in the region 1000-1300 cm^{-1} [43-46]. For the investigated molecule, the observed medium strong band was found at 1373 cm mean while the calculated value was observed at 1378 cm^{-1}. Further, The B-OH bending vibration was observed in the range of 1039-1017 cm^{-1} while in the target molecules there are two OH bending modes but only one OH bending weak band was observed at 1046 cm^{-1} and another BOH band was not present in the FT-IR spectrum.. In general, the mentioned values agree.

4.3.5 OH vibrations:

In the O–H region, very strong and broad bands in the spectra of some boronic acid molecules occur at ca 3300 cm−1. The assignment of these bands to O–H stretching vibrations is straightforward. In the spectra of phenylboronic acid [47] pentafluorophenylboronic acid [48] and 3- and 4-pyridineboronic acid [49] n-butylboronic acid [50] absorption bands at 3280,

3467, 3410, 3320 and 3306 cm−1 were assigned, which is typical for O–H bonded hydroxyl groups. The strength and broadening wavenumbers of these bands suggest that intramolecular hydrogen bonding occurs in different environments of boronic acids. In accordance with the above conclusion, the two O–H stretching vibrations occur at 3443 and 3397 cm−1 in the FT-IR spectrum. These two are pure stretching modes confirmed from the PED percentage (100%).

Table 3: complete assignments of fundamental vibrations of 4IQBA by normal mode analysis based on SQM force field calculations using B3LYP/6-311++G**

No	Experimental (cm^{-1}) FT-IR	Symmetry species	Scaled frequencies (cm^{-1})	Un-scaled frequencies (cm^{-1})	Intensity I_{IR}[b]	Characterization of normal modes with PED (%)[c]
1	--	A'	3480	3864	21.81	νOH (100)
2	3450vs	A'	3467	3849	9.72	νOH (100)
3	3178w	A'	3143	3249	2.28	νCH (99)
4	3090w	A'	3098	3202	13.13	νCH (99)
5	3084w	A'	3092	3197	6.64	νCH (99)
6	3070w	A'	3080	3184	10.71	νCH (99)
7	3056w	A'	3071	3176	0.389	νCH (99)
8	3029w	A'	3030	3133	13.92	νCH (99)
9	1675vw	A'	1673	1674	11.14	νCC (65), βCH (18)
10	1628ms	A'	1624	1626	17.16	νCN (37), νCC (30), βCH (24)
11	1608w	A'	1616	1617	21.25	νCN (60), βCH (14)
12	1545w	A'	1546	1549	37.68	νCC (43), βCH (37), νCN (10)
13	1497ms	A'	1492	1495	3.11	βCH (48), νCC (38)
14	1459w	A'	1447	1452	32.97	βCH (35), νCC (24), νCN (14)
15	1420ms	A'	1429	1433	2.88	βCH (59), νCC (23)
16	1402w	A'	1410	1409	10.45	νCC (82)
17	1380ms	A'	1386	1394	86.82	νBOas (46), νCN (13), βCH (10), νCC (10)
18	1373ms	A'	1380	1383	89.07	νBOss (34), νCB (21), βCH (19), νCN (11), βOH (11), νCC (10)
19	1352w	A'	1351	1353	27.30	νCC (42), βCH (19), νBOas (18), νCN (15)
20	1284w	A'	1284	1287	10.88	βCH (54), νCC (26), βR2tri (11)
21	1266w	A'	1258	1260	14.51	νCC (57), βCH (22), βBR1tri (11)
22	1252ms	A'	1250	1252	6.93	βCH (35), νCC (30), νCN (10)
23	1190w	A'	1192	1195	2.7	βCH (71), νCC (18)
24	1169w	A'	1167	1170	0.67	βCH (53), νCC (29), βR2tri (10)
25	1140w	A'	1139	1139	0.63	βCH (55), νCN (26), νCC (10),
26	1083w	A'	1053	1053	3.63	βCH (78), νCC (19)
27	1046w	A'	1041	1045	60.33	βOH (39), βR1tri (20), νBOss (12), νCB (11)
28	1007w	A"	1017	1007	0.05	ωCH (86), τR1tri (12)
29	995w	A"	985	993	0.002	ωCH (91)
30	--	A'	979	985	53.78	βOH (37),βR1tri (23), βR2tri (18), νBOss (12)
31	981w	A"	975	973	1.42	ωCH (91)
32	939w	A'	942	944	82.41	βOH (97)
33	914ms	A"	923	939	4.20	ωCH (85), τR2tri (12)
34	880w	A"	888	887	0.75	ωCH (81), τR1tri (10)
35	856ms	A'	865	866	3.51	βR2sym(39), νCC (12), βR1tri (10),νBOss (10)
36	819w	A'	811	813	3.40	βR2tri (23), νCC (21), βR1tri (17), βR2asy (16)
37	795w	A"	799	807	3.14	τR1tri (46), τR2tri (28), ωCH (15)
38	780vw	A"	772	773	19.53	ωCH (82), τR1tri (10)
39	685w	A"	693	695	3.62	βR1sym (35), νCC(20), βR2sym(11)
40	676w	A"	675	680	5.34	ωOC (32), τR1tri (18), ωCB (17), τR2tri (11)
41	646ms	A"	639	642	3.41	τR2tri (34), ωOC (18), τR1tri (15), ωCH(12)
42	573vw	A'	579	583	14.53	βR1asy (32), βR2sym (24), βBO2 (19)
43	557w	A'	553	557	4.20	βR1tri (39), νCC (19), βBC (12), βCBO (10)
44	543w	A"	552	550	100	τOBOH (49), τBUTT (13), τR2sym (13)
45	511w	A'	513	516	13.28	βR2asy (32), βBO2 (27), βR1asy (22)
46	492vw	A"	499	497	15.46	τR1asy (36), τOBOH (18), τBUTT (12), ωCH (10), τR2asy (10)
47	480vw	A"	463	463	7.19	τR1sym (45), τR2asy (17), ωCH (15)
48		A'	439	443	0.64	βBC (30), νCC (18), βR2asy (13), βCBO (13), βR1asy (10), βR2sym (10)
49		A"	385	386	5.95	τR2sym (33), τR1asy (29), ωCB (15)
50		A"	380	374	2.40	τCBOH (91)
51		A'	332	335	1.64	βBO2 (30), βR2asy (22), νCB (21), βCBO (10)
52		A'	305	308	2.642	βCBO(57), νCC (13), βR1asy (10)
53		A"	207	208	0.721	τR2asy (34), τR1sym (21), ωCB (15)
54		A'	175	178	0.16	βBC (73), βCBO (18)

55		A'	174	177	1.28	βBC (73), βCBO (18)
56		A"	92	92	1.66	ωCB (25),τR2asy(18), τR2sym (16),τR1sym(13)
57		A"	5	6	0.0005	τOBCC (52), τCBOH (17), ωOC (14)

[a] Abbreviations: ν, stretching; ß, in plane bending; ω, out of plane bending; τ, torsion, ss, symmetrical stretching, as, asymmetrical stretching, sc, scissoring, wa, wagging, twi, twisting, ro, rocking, ipb, in-plane bending, opb, out-of -plane bending; tri, trigonal deformation, sym, symmetrical deformation, asy, asymmetric deformation, butter, butterfly, ar, aromatic, sub, substitution, vs, very strong; s, strong; ms, medium strong; w, weak; vw, very weak.
[b] Relative IR absorption intensities normalized with highest peak absorption equal to 100.
[c] Only PED contributions ≥10% are listed.

4.4 NBO analysis:

In order to know the intra and inter molecular bonding interactions within the molecule NBO analysis was carried out to the titled compound. It also gives information about the charge transfer, conjugative interactions and stabilization energy $E^{(2)}$ in the molecule. If the stabilization energy was increases, then the interactions between electron acceptors and electron donors of the molecule were also increases, this is due to when stabilization energy increases the more conjugation with in the molecule which results the enhancement of donating nature of electron donors to electron acceptors. . The second order Fock matrix was carried out to evaluate the donor–acceptor interactions in the NBO analysis [51]. Some electron donor orbital, acceptor orbital and the interacting stabilization energy resulting from the second-order micro disturbance theory is reported [52, 53]. The result of interaction is a loss of occupancy from the concentration of electron NBO of the idealized Lewis structure into an empty non-Lewis orbital. For each donor (i) and acceptor (j), the stabilization energy $E(^2)$ associated with the delocalization i→j is estimated as

$$E(2)= - n_\sigma \frac{\langle \sigma|F|\sigma \rangle^2}{\varepsilon_\sigma^* - \varepsilon_\sigma} = - n_\sigma \frac{F_{ij}^2}{\Delta E} \qquad (2)$$

Where, $\langle \sigma|F|\sigma \rangle^2$ or F^2_{ij} is the Fock matrix element i and j NBO orbitals, ε_σ^* and ε_σ are the energies of σ and σ* NBOs and n_σ is the population of the donor σ orbital. The NBO analysis has been performed on the compound using NBO 3.1 program as implemented in the Gaussian 09W package at the DFT-B3LYP/6-311++G** level of theory. Stabilization energies of the titled molecule were calculated by applying the second order perturbation theory analysis. The stabilization interaction between the donor and acceptor bonds was shown in Table 4. From the table we observed that the interaction between lone pair of N9 to σ * of C5-C10 and C7-C8 has the stabilization energy 10.90 and 9.53 kJ/mol respectively, which shows the highest stabilization energy with in the molecule. Thereafter, the interaction between σ of B11-O12 to σ * of C7-C8 and σ of B11-O13 to σ * of C6-C7 shows the stabilization energy 1.14 and 1.55 kJ/mol respectively which represents the lowest stabilization energy with in the molecule. The interaction between π of C1-C2 to π* of C3-C4 shows the stabilization energy 17.13 kJ/mol which was another significant interaction with in the molecule. Which was the most significant interaction due to π → π* transition increases the stabilization.

Table 4: The Second-order perturbation energies $E^{(2)}$ (in (kJ mol^{-1}) corresponding to the important hyper conjugative interactions (donor-acceptor) in 4IQBA

Donor(i)	Type	Ed/e	Acceptor(j)	Type	Ed/e	$E^{(2)a}$ (kJ mol^{-1})	E(i)-E(j)[b] (a.u)	f(i,j)[c] (a.u)
C1-C2	σ	1.98137	C1-C6	σ *	0.02269	2.73	1.25	0.052
	σ		C2-C3	σ *	0.01706	2.47	1.25	0.050
	σ		C3-H16	σ *	0.01237	2.04	1.18	0.044
	σ		C6-C7	σ *	0.02738	3.26	1.25	0.057
C1-C2	π	1.72552	C3-C4	π *	0.24840	17.13	0.29	0.063
C1-C6	σ	1.97623	C1-C2	σ *	0.01396	2.55	1.28	0.051
	σ		C2-H15	σ *	0.01203	2.28	1.15	0.046
	σ		C5-C6	σ *	0.03227	2.94	1.22	0.053
	σ		C5-C10	σ *	0.03416	2.48	1.21	0.049
	σ		C6-C7	σ *	0.02738	3.32	1.22	0.057
C1-H14	σ	1.97936	C2-C3	σ *	0.01706	4.17	1.06	0.059
	σ		C5-C6	σ *	0.03227	4.00	1.06	0.058
C2-C3	σ	1.98063	C1-C2	σ *	0.01396	2.47	1.29	0.051
	σ		C1-H14	σ *	0.01708	2.31	1.18	0.047
	σ		C3-C4	σ *	0.01355	2.60	1.29	0.052
	σ		C4-H17	σ *	0.01371	2.78	1.15	0.051
C2-H15	σ	1.98263	C1-C6	σ *	0.02269	4.33	1.07	0.061
	σ		C3-C4	σ *	0.24840	3.27	1.13	0.054
C3-C4	σ	1.98139	C2-C3	σ *	0.01706	2.42	1.26	0.049
	σ		C2-H15	σ *	0.01203	2.03	1.18	0.044
	σ		C4-C5	σ *	0.02181	2.85	1.26	0.054
	σ		C5-C10	σ *	0.03416	2.97	1.25	0.055
C3-C4	π	1.98139	C1-C2	π *	0.23900	17.60	0.30	0.065
C3-H16	σ	1.98249	C1-C2	σ *	0.01396	3.26	1.13	0.054
	σ		C4-C5	σ *	0.02181	4.01	1.07	0.059
C4-C5	σ	1.97537	C3-C4	σ *	0.01355	2.58	1.29	0.052
	σ		C3-H16	σ *	0.01237	2.54	1.16	0.049

	σ		C5-C6	σ *	0.03227	3.37	1.22	0.057
	σ		C5-C10	σ *	0.03416	2.70	1.22	0.051
C4-H17	σ	1.98145	C2-C3	σ *	0.01706	3.74	1.07	0.057
	σ		C5-C6	σ *	0.03227	4.39	1.07	0.061
C5-C6	σ	1.96822	C1-C6	σ *	0.02269	2.50	1.22	0.049
	σ		C4-C5	σ *	0.02181	3.07	1.22	0.055
	σ		C5-C10	σ *	0.03416	2.55	1.21	0.050
	σ		C6-C7	σ *	0.02738	2.80	1.21	0.052
	σ		C7-B11	σ *	0.03205	2.19	1.14	0.045
C5-C10	σ	1.98176	C1-C6	σ *	0.02269	2.54	1.24	0.050
	σ		C4-C5	σ *	0.02181	2.97	1.24	0.054
	σ		C5-C6	σ *	0.03227	2.87	1.23	0.053
C6-C7	σ	1.97240	C1-C6	σ *	0.02269	3.12	1.22	0.055
	σ		C4-C5	σ *	0.02181	2.62	1.22	0.051
	σ		C5-C6	σ *	0.03227	2.77	1.21	0.052
	σ		C7-C8	σ *	0.02796	2.90	1.26	0.054
	σ		C7-B11	σ *	0.03205	2.46	1.14	0.047
	σ		C8-H18	σ *	0.02092	2.35	1.17	0.047
C7-C8	σ	1.98089	C1-C6	σ *	0.02269	3.77	1.25	0.061
	σ		C6-C7	σ *	0.02738	3.42	1.24	0.058
	σ		C7-B11	σ *	0.03205	2.81	1.17	0.051
C7-B11	σ	1.95435	C5-C6	σ *	0.03227	3.69	1.07	0.056
	σ		C8-N9	σ *	0.01880	5.75	1.05	0.070
	σ		O12-H20	σ *	0.01015	2.63	0.96	0.045
	σ		O13-H21	σ *	0.01160	2.70	0.96	0.046
C8-N9	σ	1.98531	C10-H19	σ *	0.02410	3.03	1.26	0.055
C8-H18	σ	1.98157	C6-C7	σ *	0.02738	4.39	1.05	0.061
	σ		N9-C10	σ *	0.01176	4.19	1.09	0.060
C10-H19	σ	1.98200	C5-C6	σ *	0.03227	4.30	1.07	0.061
	σ		C8-N9	σ *	0.01880	4.91	1.04	0.064
B11-O12	σ	1.99593	C6-C7	σ *	0.02738	1.55	1.46	0.043
B11-O13	σ	1.99624	C7-C8	σ *	0.02796	1.14	1.51	0.037
O12-H20	σ	1.98596	C7-B11	σ *	0.03205	3.08	1.21	0.055
O13-H21	σ	1.98589	C7-B11	σ *	0.03205	3.23	1.21	0.056
N9	LP	1.92590	C5-C10	σ *	0.03416	10.90	0.87	0.088
N9	LP	1.92590	C7-C8	σ *	0.02796	9.53	0.92	0.085
O12	LP	1.96353	B11-O13	σ *	0.02792	7.70	0.98	0.078
O13	LP	1.99997	B11-O12	σ *	0.02500	7.34	0.99	0.076

[a] $E^{(2)}$ means energy of hyper conjugative interaction (stabilization energy).
[b] Energy difference between donor and acceptor i and j NBO orbitals.
[c] F(i,j) is the Fock matrix element between i and j NBO orbitals.

4.5 Frontier Molecular Orbitals:

FMOs consist of the highest occupied molecular orbital (HOMO) and the lowest unoccupied molecular orbital (LUMO). Frontier molecular orbitals show us the reactive position in the conjugated system and different types of reactions occurred in the reactive site [54]. HOMO-LUMO energy gap also presents that the charge transfer within the molecule. Generally absorption maxima in UV-Vis spectrum was due to the transfer of electron from Highest occupied molecular orbital to lowest unoccupied molecular orbital. In order to know the energies of Frontier molecular orbitals and their energy gap, we performed Frontier Molecular orbital analysis to the titled compound by using DFT/B3LYP/6-311++G** basis set. So from the results, The HOMO energy was -5.99 eV and the LUMO energy was -1.395 eV. The energy gap between the HOMO and LUMO was 4.600 eV. The First exited state and ground state energy levels diagram presented in fig. 4. Thereafter, ionization energy and electron affinity can be showed in terms of HOMO and LUMO orbital energies as $I = -E_{HOMO}$ and $A = -E_{LUMO}$ [55] Then the calculated values global reactive descriptors were reported in the Table 5.

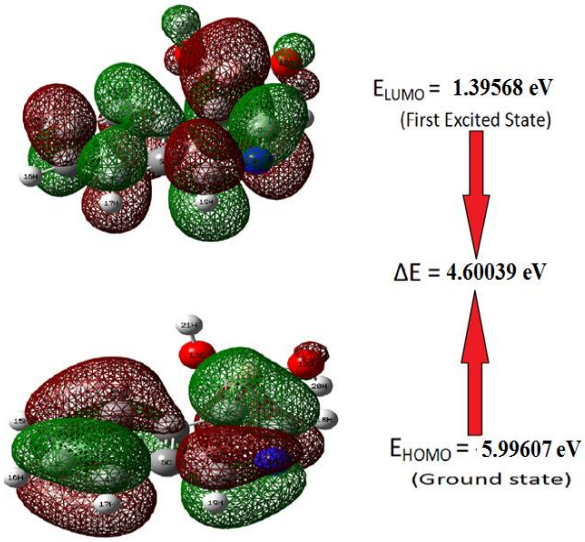

Fig. 4: The visualization of frontier molecular orbitals (HOMO—MO: 45, LUMO—MO: 46) of 4IQBA

Table 5: Frontier molecular orbital quantum chemical parameters for 4IQBA

Property	DFT/B3LYP/6-311++G**
Total energy (eV)	-15624.297
E_{HOMO} (eV)	-5.99607
E_{LUMO} (eV)	-1.39568
E_{HOMO}-E_{LUMO} (eV)	4.60039
Ionization energy (I)	5.99607
Electron Affinity (A)	1.39568
Electronegativity (χ)eV	3.69587
Chemical hardness(η)eV	2.30019
Chemical potential(ρ)	-3.69587
Electrofilicity index (ω) eV	2.96920
Global Softness (σ)eV	0.43474
Total energy change(ΔE_T) eV	-0.57504
Dipole moment(D)	3.9736

4.6 Electronic absorption spectrum:

The absorption spectroscopy has been widely used to understand the electronic transitions as well as optical properties of compounds [56]. In order to know the positions of experimental and theoretical absorption maxima (λ_{max}), excitation energies (E), oscillator strength (f) and assignments of the suitable transitions for the titled compound, we have to calculate the electronic absorption spectrum by using TD-DFT method based on the B3LYP/6-311++G** level in gas phase medium and the results are reported . The five transitions along with oscillator strengths and excitation energies are shown in Table 6. The experimental and theoretically simulated UV-Visible spectrum was presented in Fig 5.

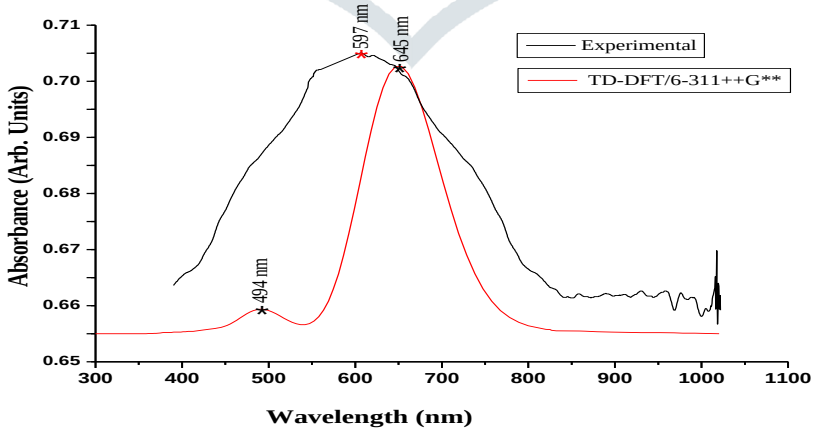

Fig. 5: Theoretical and experimental absorption spectrum of 4-IQBA

Table 6: The UV–Vis excitation energy and oscillator strength for 4-IQBA calculated by TD-DFT/B3LYP/6-311++G** method.

No.	Exp. Wavelength (nm)	Energy (cm^{-1})	Wavelength (nm)	Osc. Strength	Symmetry	Major contributions
1	597	26728.59	645.267	0.0008	Singlet-A	H-1->LUMO (97%)
2		30471.84	610.083	0.11	Singlet-A	HOMO->LUMO (82%)
3		35441.05	592.158	0.01	Singlet-A	H-2->LUMO (63%), HOMO->L+1 (38%)
4	--	38201.1	494.287	0.0015	Singlet-A	H-1->L+1 (92%)H-1->L+2 (2%)
5		39202.04	436.088	0.0001	Singlet-A	H-3->LUMO (95%) H-3->L+2 (3%)

4.8 Electronic properties:

The non- linear optical (NLO) properties of an organic compound have been used in the field of fiber-optic communication, optical switching and optical data storage in photonics technology [57]. Most of the in organic molecules, π-conjugated molecules were substituted with an electron-donating group and an electron-accepting group which was increases the second order hyperpolarizability causes enhancement of non-linearity with in the molecule. The non-linear optical properties of the molecule was calculated by using B3LYP/6-311++G** basis set. The polarizability and static first order hyperpolarizabilities tensors i.e. (α_{xx}, α_{xy}, α_{yy}, α_{xz}, α_{yz}, α_{zz} and β_{xxx}, β_{xxy}, β_{xyy}, β_{yyy}, β_{xxz}, β_{xyz}, β_{yyz}, β_{xzz}, β_{yzz}, β_{zzz}) can be find out from the results of Gaussian output file. The complete set of formulas for calculating the magnitude of total static dipole moment μ, the mean polarizability α_0, the anisotropy of the polarizability Δα and the mean first hyperpolarizability β_0, using the x, y, z components from Gaussian 09W output is as follows

$$\mu = \mu^2_x + \mu^2_y + \mu^2_z \quad (3)$$

$$\alpha_o = \frac{\alpha_{xx} + \alpha_{yy} + \alpha_{zz}}{3} \quad (4)$$

$$\Delta\alpha = 2^{-1/2}[(\alpha_{xx} - \alpha_{yy})^2 + (\alpha_{yy} - \alpha_{xx})^2 + 6\alpha^2_{xx}]^{1/2} \quad (5)$$

$$\beta = (\beta^2_x + \beta^2_y + \beta^2_z)^{1/2} \quad (6)$$

And

$$\beta_x = \beta_{xxx} + \beta_{xyy} + \beta_{xzz} \quad (7)$$

$$\beta_y = \beta_{yyy} + \beta_{xxy} + \beta_{yzz} \quad (8)$$

$$\beta_z = \beta_{zzz} + \beta_{xxz} + \beta_{yyz} \quad (9)$$

All the reported values are reported in Atomic units (A.U), so the calculated values have been converted into electrostatic units (esu) (α: 1a.u= 0.1482 x 10^{-24} esu, β: 1 a.u = 8.6393×10^{-33} esu) and results are reported in Table. 7. The calculated average polarizability and exact polarizability of the molecule were 15.73496 x 10^{-24} esu and 35.75001 x 10^{-24} esu. The calculated value of dipole moment was 1.432 Debye. In this title molecule, the first order hyperpolarizability value (β) is equal to 1.441937 x 10^{-30} esu. From these results we can concluded that titled compound was active and dynamic in all coordinates. Thereafter, due to significant values of polarizability and hyperpolarizability, the investigated compound has capable to bind with another molecule with less amount of binding energy and can be used to produce NLO material for photonics technology.

Table 7: calculated values of dipole moment μ_t (in Debye), polarizability, α_t (in 1.4882 x 10^{-24} esu) and first order hyperpolarizability, β_t (in 10^{-30} esu) of 4IQBA

μ and α components	B3LYP/6-311++G**	β components	B3LYP/6-311++G**
μ_x	-0.3500852	β_{xxx}	-26.5530572
μ_y	-0.0168122	β_{xxy}	13.8003383
μ_z	1.1442045	β_{xyy}	-25.8156374
μ(D)	1.4320455	β_{yyy}	-0.1598939
α_{xx}	126.9919008	β_{xxz}	-130.5256939
α_{xy}	-1.5860262	β_{xyz}	0.641099
α_{yy}	41.533373	β_{yyz}	-21.7696639
α_{xz}	-3.0003294	β_{xzz}	-45.6652228
α_{yz}	1.3563665	β_{yzz}	-16.4139999
α_{zz}	149.9533619	β_{zzz}	16.1824991
α (esu)	15.73496 x 10^{-24} esu	β_{total} (esu)	1.44937×10^{-30} esu
Δα	35.75001 x 10^{-24} esu		

4.9 Molecular electrostatic potential map:

The molecular electrostatic potential (MESP) is best widely used method for identifying the intramolecular and intermolecular interactions with in the molecule. It also gives information about the electrophilic and nucleophilic regions and

hydrogen bonding interactions within the investigated molecule. The molecular electrostatic potential (MESP) V(r) at a point r by reason of a molecular system with nuclear charges {ZA} positioned at {RA} and the electron density ρ(r) is given by

$$V(r) = \Sigma^{N}{}_{A} [(Z_A / |r-R_A|) - \int \rho(r')d^3r'/|r-r'| \quad (10)$$

Where, N shows the entire number of nuclei in the titled molecule and the two terms indicate to the bare nuclear potential and the electronic contributions of the molecule. The balance of these two terms brings about the effective localization of electron-rich regions in the molecular system. The MESP topography is mapped by examining the Eigen value of the Hessian matrix at the point where the gradient V(r) vanishes. The electrostatic potential is a physical property of a molecule related to how a molecule is first "seen" or "felt" by another approaching species. A portion of a molecule that has a negative electrostatic potential will be susceptible to electrophilic attack - the more negative the better. It is not as straightforward to use electrostatic potentials to predict nucleophilic attack. MESP map was represented in fig. 6. From figure 6 it was observe that negative electro potential is located over Oxygen atoms of the Boronic acid group, further positive electrostatic potential was developed over the Hydrogen atoms.

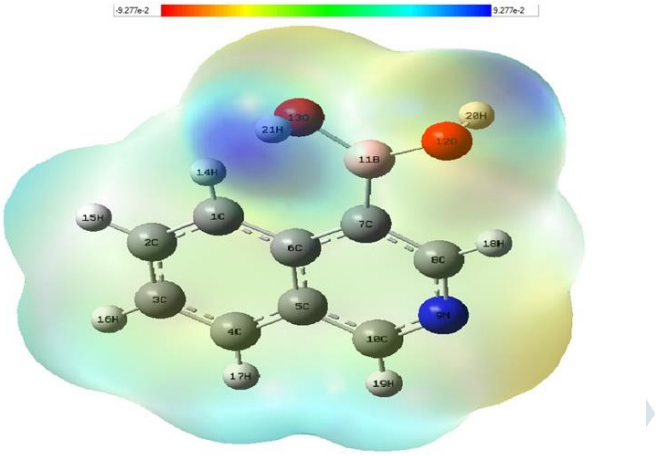

Fig. 6: Total electron density mapped with electrostatic surface potential (MESP) of 4-IQBA

V. Conclusion:

The optimize structural parameters, vibrational, electronic, fluorescence spectroscopic and Quantum chemical studies of 4IQBA was studied theoretically and experimentally by using FT-IR, UV-Visible and Fluorescence spectrum. The main important results obtained from present investigation are the most optimized structural parameters of the titled compound obtained from the B3LYP method with 6-311++G** basis set shows smallest deviation between the experimental theoretical values. All the bands of the investigated compound observed in the FT-IR spectrum was assigned by using PED method. The analysis of di pole moment, polarizability and hgyperpolarizability properties described the titled compound was used to produce NLO material for photonics technology. The HOMO, LUMO energies and small band gap between HOMO-LUMO shows the titled compound was stable, high chemical reactivity and low kinetic stable. NBO analysis describes the charge transfer, strong intramolecular hyperconjugative interaction within the molecule and stability of the molecule. The MESP map of the investigated molecule shows the negative electrostatic potential was located over the oxygen atoms of the Boronic acid group. The thermodynamic parameters of the titled compound also determined at different temperatures.

Acknowledgement:

The corresponding author, A.Veeraiah is highly grateful to Science and Engineering Research Board, Department of Science and Technology, Government of India (Project code- SB/EMEQ/2014) and Management of D.N.R.College Association for their financial support and cooperation respectively. Further, the authors are highly grateful to Prof. T. Sundius for Molvib program.

References:

[1] Gilchrist, T.L. (1997) Heterocyclic Chemistry (3rd ed.). Essex, UK: Addison Wesley Longman.
[2] Harris, J.; Pope, W.J. (1922) Journal of the Chemical Society volume 121, pp. 1029–1033.
[3] Katritsky, A.R.; Pozharskii, A.F. (2000). Handbook of Heterocyclic Chemistry (2nd ed.). Oxford, UK: Elsevier.
[4] Katritsky, A.R.; Rees, C.W.; Scriven, E.F. (Eds.). (1996). Comprehensive Heterocyclic Chemistry II: A Review of the Literature 1982–1995 (Vol. 5). Tarrytown, NY: Elsevier
[5] Nagatsu, T. "Isoquinoline neurotoxins in the brain and Parkinson's disease" Neuroscience Research (1997) volume 29, pp. 99–111.
[6] O'Neil, Maryadele J. (Ed.). (2001). The Merck Index (13th ed.). Whitehouse Station, NJ: Merck.
[7] W.A. Creasey, (1979) Biochemical effects of berberine, Biochem. Pharmacol. 28 1081-1084.
[8] J. Liu, P. Chan, Y. Chen, B. Tomlinson, S. Hong, (1999) The antihypertensive effect of the berberine derivative 6-protoberberine in spontaneously hypertensive rats, Pharmacology
[9] T.C. Birdsall, Berberine(1997): Altern. Med. (Rev. 2)94–103.
[10] J. Zhou, S. Zhou, J. Tang, K. Zhang, L. Guang, Y. Huang, Y. Xu, Y. Ying, L. Zhang, D. Li, (2009) Eur. J. Pharmacol. 606, 262–268.
[11] K. Zee-Cheng, K. Paull, (1974).J. Med.
[12] R. Gupta, W. Murray, R. Gupta, (1988) Br. J. Cancer. 58, 441–7
[13] Yoon, T.; De Lombaert, S.; Brodbeck, R.; Gulianello, M.; Chandrasekhar, J.;Horvath, R. F.; Ge, P.; Kershaw, M. T.; Krause, J. E.; Kehne, J.; Hoffman, D.; Doller, D.; Hodgetts, K. J. Bioorg. 2008, Med. Chem. Lett. 18, 891–896.
[14] Örtqvist, P.; Peterson, S. D.; Åkerblom, E.; Gossas, T.; Sabnis, Y. A.; Fransson, R.; Lindeberg, G.; Danielson, U. H.; Karlén, A.; Sandström, A. Bioorg. 2007, Med.Chem. 15, 1448–1474.

[15] Trotter, B. W.; Nanda, K. K.; Kett, N. R.; Regan, C. P.; Lynch, J. J.; Stump, G. L.; Kiss, L.; Wang, J.; Spencer, R. H.; Kane, S. A.; White, R. B.; Zhang, R.; Anderson, K. D.; Liverton, N. J.; McIntyre, C. J.;Beshore, D. C.; Hartman, G. D.; Dinsmore, 2006, C. J. J. Med. Chem. 49, 6954–6957
[16] Ribeiro da Silva, M. A. V.; Matos, M. A. R.; Amaral, L. M. P. F. 2005, J.Chem. Thermodyn. 37, 1312−1317.
[17] Ribeiro da Silva, M. A. V.; Matos, M. A. R.; Amaral, L. M. P. F. 1995, J.Chem. Thermodyn. 27, 1187−1196.
[18] L. Strekowski, J.L. Mokrosz, V.A. Honkan, A. Czarxy, M.T. Ceyla, R.L. Wydra, S.E.
Patterson, R.F. Schinazi, (1991) J. Med. Chem. 34 ,1739.
[19] P.G. Bray, S.R. Hawley, S.A. Ward, (1996) Mol. Pharmacol. 50 ,1551.
[20] A. Sparatore, N. Basilico, M. Casagrande, S. Parapini, D. Taramelli, R. Brun, S.
Wittlin, F. Sparatore, Bioorg. (2008) Med. Chem. Lett. 18 ,3737.
[21] C.Y. Watson, W.J.D. Whish, M.D. Threadgill, Bioorg. (1998) Med.Chem. 6 ,721.
[22] A.W. White, R. Almassy, A.H. Calvert, N.J. Curtin, R.J. Griffin,Z. Hostomsky, K. Maegley, D.R. Newell, S. Srinivasan, B.T.Goldings, (2000) J. Med. Chem. 43 ,4048.
[23] M. J. Frisch, G. W. Trucks, H. B. Schlegel, G. E. Scuseria, M. A. Robb, J. R. Cheeseman, G. Scalmani, V. Barone, B. Mennucci, G. A. Petersson, H. Nakatsuji, M. Caricato, X. Li, H. P. Hratchian, A. F. Izmaylov, J. Bloino, G. Zheng, J. L. Sonnenberg, M. Hada, M. Ehara, K. Toyota, R. Fukuda, J. Hasegawa, M. Ishida, T. Nakajima, Y. Honda, O. Kitao, H. Nakai, T. Vreven, J. A. Montgomery, Jr., J. E. Peralta, F. Ogliaro, M. Bearpark, J. J. Heyd, E. Brothers, K. N. Kudin, V. N. Staroverov, R. Kobayashi, J. Normand, K. Raghavachari, A. Rendell, J. C. Burant, S. S. Iyengar, J. Tomasi, M. Cossi, N. Rega, J. M. Millam, M. Klene, J. E. Knox, J. B. Cross, V. Bakken, C. Adamo, J. Jaramillo, R. Gomperts, R. E. Stratmann, O. Yazyev, A. J. Austin, R. Cammi, C. Pomelli, J. W. Ochterski, R. L. Martin, K. Morokuma, V. G. Zakrzewski, G. A. Voth, P. Salvador, J. J. Dannenberg, S. Dapprich, A. D. Daniels, Ö. Farkas, J. B. Foresman, J. V. Ortiz, J. Cioslowski, and D. J. Fox, Gaussian 09 (Gaussian, Inc., Wallingford CT, (2009)
[24] G. Fogarasi, X. Zhou, P.W. Taylor, P. Pulay, (1992) J. Am. Chem. Soc. 114 ,8191.
[25] G. Rauhut, P. Pulay, (1995) J. Phys. Chem. 99 ,3093.
[26] T. Sundius, J. Mol. Struct. 218 (1990) 321; MOLVIB: A Program for Harmonic force field calculations, QCPE Program No. 604
[27] T. Sundius, (2002) Vib. Spectrosc. 29 , 89.
[28] Z.-X. Miao, M. Shao, M.-X. Li, (2007) Acta Crystallogr. Sect. E Struct. Reports Online.63
[29] S.J. Rettig, J. Trotte, Can. J. Chem. 55 (1977) 3071–3075
[30] P. Pulay, G. Fogarasi, F. Pang, and J. E. Boggs, (1979) J. Am. Chem. Soc. 101 ,2550
[31] G. Fogarasi, X. Zhou, P.W. Taylor, P. Pulay, (1992)J. Am. Chem. Soc. 114
[32] Keresztury G, Raman spectroscopy: Theory in Hand book of Vibrational spectroscopy, Chalmers J M & Giffith P R, John Wiley & Sons Ltd, (2002)
[33] Silverstein R M, Bassler G C & Morrill T C, spectrometric Identification of Organic compounds, 5th ed., Chichester, John Wiley, (1991)
[34] Socrates G, Infrared Raman Characteristic Group Frequencies- Tables and charts, third ed, Wiley, New York, (2001)
[35] V. Arjunan, S. Thillai Govindaraja, A. Jayapraksh, S. Mohan, (2013) Spectrochim. Acta - Part A Mol. Biomol. Spectrosc. 107 62–71.
[36] S. Sebastian, S. Sylvestre, N. Sundaraganesan, M. Amalanathan, S. Ayyapan, K.Oudayakumar, B. Karthikeyan, (2013) Spectrochim. Acta - Part A Mol. Biomol. Spectrosc. 107 ,167–178.
[37] K.J.D. Silverstein M.Robert, Webster X. Francis, (2005) Spectrometric Identification of Organic Compounds, Org. Chem. 1–550.
[38] V. Arjunan, S. Thillai Govindaraja, S. Subramanian, S. Mohan, (2013) J. Mol. Struct. 1037, 73–84.
[39] V. Arjunan, S. Thillai Govindaraja, P. Ravindran, S. Mohan, (2014) Spectrochim. Acta - Part A Mol.Biomol. Spectrosc. 120, 473–488.
[40] Kurt, M. 2008, J.Mol. Struct. 874, 159–169.
[41] Smith, G.T.; Howard, J.A.K.; Wallis, J.D. 2001, Phys. Chem. Chem. Phys. 3, 4501–4507
[42] Karabacak, M.; Sinha, L.; Prasad, O.; Asiri, A.M.; Cinar, M. 2013, Spectrochim. Acta Part. A Mol. Biomol. Spectrosc. 115, 753–766
[43] Alver, Ö.; Parlak, C. 2010, Vib. Spectrosc. 54, 1–9
[44] Erdogdu, Y.; Tahir Güllüoglu, M.; Kurt, M. 2009, J. Raman Spectrosc. 40, 1615–1623
[45] Tian, S.X.; Xu, K.Z.; Huang, M.-B.; Chen, X.J.; Yang, J.L.; Jia, C.C. 1999, J. Mol. Struct. THEOCHEM 469, 223–227
[46] Zarandi, M.; Salimi Beni, A. 2016, J. Mol. Struct. 1119, 404–412
[47] J. A. Faniran, H. F. Shurvell, Can. 1968, J. Chem. 46, 2089
[48] M. Kurt, 2008, J. Mol. Struct. 874, 159
[49] M. Kurt, T. R. Sertbakan, M. Ozduran, 2008, Spectrochim. Acta 70A, 664
[50] M. K. Cyranski, A. Jezierska, P. Klimentowska, J. J. Panek, G. L. Zukowska, A. Sporzynski, J. Chem. Phys. 2008, 128, 124512
[51] M. Sarafran, A. Komasa, E.B. Adamska, (2007) J. Mol. Struct. (Theochem.) 827, 101
[52] C. James, A. AmalRaj, R. Reghunathan, I. Hubert Joe, V.S. JayaKumar, J. Raman (2006) Spectrosc. 37, 1381
[53] L.J. Na, C.Z. Rang, Y.S. Fang, J. Zhejiang (2005) Univ. Sci. 6B, 584
[54] I. Fleming, Frontier Orbitals, Organic Chemical Reactions, Wiley, London, 1976
[55] T.A. Koopmans, Physica, 1933, 1, 104-113
[56] Fazl-i-Sattar, Z. Ullah, Ata-ur-Rahman, A. Rauf, M. Tariq, A.A. Tahir, K. Ayub, H. Ullah, (2015) Spectrochim. Acta Part A Mol.Biomol. Spectrosc. 141, 71–79
[57] Yunus Kaya, Veysel T. Yilmaz and Orhan Buyukgungor, 2016, Molecules 21, 52,